UNIVERSITY OF CALIFORNIA

Los Angeles

Closed-Loop Subspace Identification of a Quadrotor

A thesis submitted in partial satisfaction

of the requirements for the degree

Master of Science in Engineering

by

Andrew G. Kee

2013

ABSTRACT OF THE THESIS

Closed-Loop Subspace Identification of a Quadrotor

by

Andrew G. Kee

Master of Science in Engineering

University of California, Los Angeles, 2013

Professor Steve Gibson, Chair

Ne quo feugiat tractatos temporibus, eam te malorum sensibus. Impetus voluptua senserit id mel, lucilius adipiscing at duo. Suas noster sanctus cu pro, movet dicam intellegebat pri ad, esse utamur vulputate ut per. Admodum facilisi sea an, omittam molestiae pertinacia vim eu, et eam illud graeco. Enim persius duo ei, mea te posse congue putent.

Has ut commodo inermis definiebas. Eu pro audire fabellas. Te qui zril omnes forensibus, ius an dico tempor maiorum. Ea mel illud adipisci.

Ad vel dicant aliquip, ut eam agam constituto, no quo erant melius. Porro labores invidunt ad vel, quaeque epicurei vituperatoribus ex cum. Qui tamquam omnesque ex, essent percipitur intellegam an per. Iusto expetenda sed et.

The thesis of Andrew G. Kee is approved.

Steve Gibson, Committee Chair

University of California, Los Angeles

2013

TABLE OF CONTENTS

LIST OF FIGURES

List of Tables

Nomenclature

$\mathbb{R}$ Set of all reals

$\mathbb{Z}$ Set of all integers

A System matrix

B Input matrix

C Output matrix

D Feedforward matrix

u System input vector

y System output vector

e System innovation vector

x System state vector

v Process noise vector

w Measurement noise vector

n Number of system states

m Number of system inputs

l Number of system outputs

l Number of system outputs

σ Singular value

K Kalman filter gain

U_k Block Hankel matrix of system inputs

U_p Block Hankel matrix of past system inputs

U_f Block Hankel matrix of future system inputs

Y_k Block Hankel matrix of system outputs

Y_p Block Hankel matrix of past system outputs

Y_f Block Hankel matrix of future system outputs

X_k Block Hankel matrix of system states

E_k Block Hankel matrix of system innovation

E_f Block Hankel matrix of future system innovation

Γ_k Extended observability matrix

$\hat{\Gamma}_f$ Estimate of extended observability matrix over future horizon

G_f Toeplitz matrix of future Markov parameters of stochastic subsystem

H_f Toeplitz matrix of future Markov parameters of deterministic subsystem

f Future time horizon

p Past time horizon

$\Pi_{U_f}^{\perp}$ Orthogonal projection onto the column space of U_f

I Identity matrix

Z Instrumental variable matrix

Z_p Instrumental variable matrix constructed of past input-output data

CHAPTER 1

Introduction

Unmanned Aerial Vehicles (UAVs) have seen explosive growth in the past thirty years, performing a multitude of military and civilian tasks including surveillance, reconnaissance, armed combat operations, search and rescue, forest fire management, and domestic policing [15, 17]. A class of modern UAVs which have recently grown in popularity are quadrotors - Vertical Take Off and Landing (VTOL) vehicles powered by four rotors arranged in a cross configuration. The main advantage of the quadrotor lies in its mechanical simplicity. Adjusting the speed of one or more of the vehicle's fixed-pitch rotors provides full attitude control, eliminating the need for the swash plate mechanism found on single rotor helicopters [2, 4]. In spite of its mechanical simplicity, the quadrotor exhibits somewhat complex dynamics that are best modeled as a Multi-Input Multi-Output (MIMO) system.

Advances in MEMS sensors and light-weight high-powered lithium polymer batteries have contributed to the recent popularity of quadrotors, making them an attractive choice for research applications in flight dynamics and control, as in [5, 9, 11, 12]. One problem of particular interest is the development of mathematical models representing system dynamics based on experimentally gathered data. System identification provides a mechanism to relate this input-output data to the underlying system dynamics. Traditionally, system identification techniques have focused on developing a system model which minimizes prediction error. Identification methods of this form are commonly known as Prediction Error Methods (PEMs). PEMs have seen widespread use in both theoretical and real-world ap-

plications, but experience difficulties with MIMO systems as noted in [13, 23]. Subspace identification methods have recently grown in popularity and offer an alternative approach to the identification problem. These methods have a foundation in linear algebra and overcome the issues found in PEMs when identifying MIMO systems [8]. It is the goal of this research project to apply subspace identification techniques to a quadrotor using experimentally gathered closed-loop input and output data.
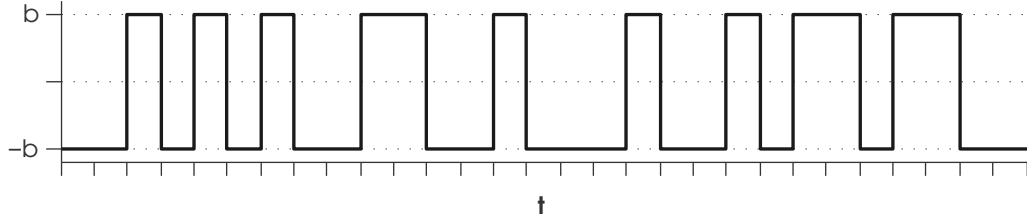
1.1 Related Work

Figure 1.1: A general Pseudo-Random Binary Sequence (PRBS).

1.2 Motivation and Contributions
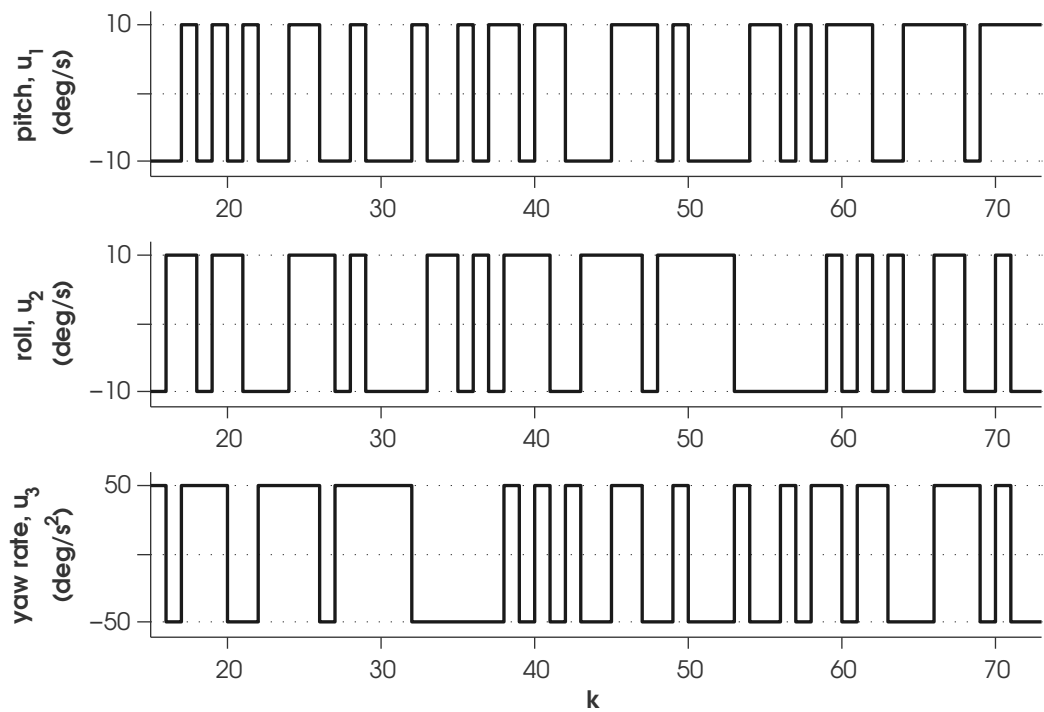
Figure 1.2: A specific Pseudo-Random Binary Sequence (PRBS) used in testing
CAPTION NEEDS MORE WORK HERE.

CHAPTER 2

Preliminaries

2.1 Notation

Let $\mathbb{R}$ be the set of reals, $\mathbb{R}^n$ the set of n-dimensional real vectors, and $\mathbb{R}^{m \times n}$ the set of real matrices. We denote vectors by lower case letter a, b, c, ... and matrices by upper case letters A, B, C, ... Transpositions of vectors and matrices are denoted by a^T and A^T, respectively. The inverse of a square matrix A is denoted A^{-1} and its Moore-Penrose pseudoinverse denoted by $A^\dagger$.

2.2 Linear Systems

2.2.1 Linear Time-Invariant Systems

A discrete time state space representation of a linear dynamical system can be written as

$$x(k+1) = Ax(k) + Bu(k) \tag{2.1a}$$

$$y(k) = Cx(k) + Du(k) \tag{2.1b}$$

where $x(k) \in \mathbb{R}^n$ is a vector of the states of the system, $u(k) \in \mathbb{R}^m$ is a vector of input signals, and $y(k) \in \mathbb{R}^l$ is a vector of output signals for $k \in \mathbb{Z}$. A, B, C, and D are the system matrices with dimensions $A \in \mathbb{R}^{n \times n}$, $B \in \mathbb{R}^{n \times m}$, $C \in \mathbb{R}^{l \times n}$, $D \in \mathbb{R}^{l \times m}$.

It is important to see that the system state is not unique. That is, there are different state representations resulting in the same input-output behavior of the
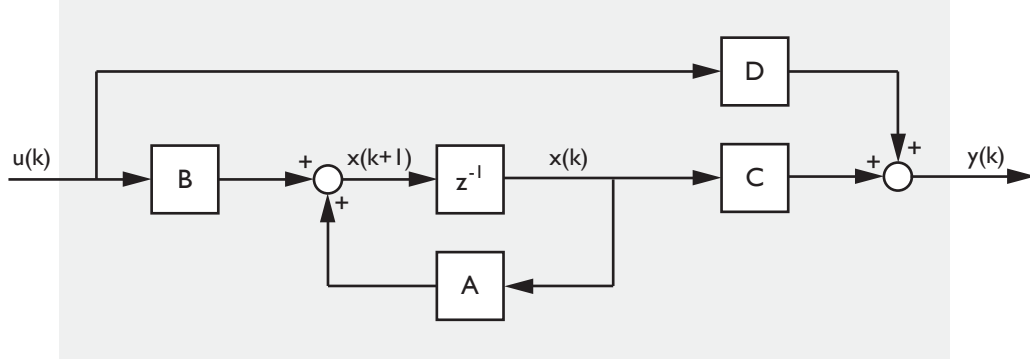
Figure 2.1: A block diagram of the state space representation of an LTI system.

system. These differing states can be related by a similarity transform T where T is a real, nonsingular matrix:

$$\tilde{x}(k) = T^{-1}x(k)$$

The state space representation of the system corresponding to the transformed state $\tilde{x}$ is given by

$$\tilde{x}(k+1) = \tilde{A}\tilde{x}(k) + \tilde{B}u(k)$$

$$y(k) = \tilde{C}\tilde{x}(k) + \tilde{D}u(k)$$

with

$$\tilde{A} = T^{-1}AT, \qquad \tilde{B} = T^{-1}B, \qquad \tilde{C} = CT, \qquad \tilde{D} = D$$

As a result of this fact, we are able to extract the system matrices to within a similarity transform from input-output data through the application of subspace identification methods.

2.2.2 Combined Deterministic-Stochastic LTI Systems

Section 2.2.1 considered the case of a purely deterministic system; that is, a system operating in a noise-free environment. In practice, this rarely happens so we will now consider the case of the combined deterministic-stochastic LTI system

operating in the presence of process and measurement noise. We append 2.1 as follows

$$x(k+1) = Ax(k) + Bu(k) + w(k) \tag{2.3a}$$

$$y(k) = Cx(k) + Du(k) + v(k) \tag{2.3b}$$

where $w(k) \in \mathbb{R}^1$ and $v(k) \in \mathbb{R}^1$ are the process and measurement noises, respectively. As is commonly done, we assume $w(k)$ and $v(k)$ are zero-mean white-noise sequences.

If the system is observable, we can design a Kalman filter to estimate the system state [7]

$$\hat{x}(k+1) = A\hat{x}(k) + Bu(k) + K\big(y(k) - C\hat{x}(k) - Du(k)\big)$$

where K is the Kalman filter gain. If we denote

$$e(k) = y(k) - C\hat{x}(k) - Du(k)$$

to be the innovation sequence, we can rewrite the combined deterministic-stochastic system in Eq. (2.3) in the following equivalent *innovation form*:

$$x(k+1) = Ax(k) + Bu(k) + Ke(k) \tag{2.4a}$$

$$y(k) = Cx(k) + Du(k) + e(k) \tag{2.4b}$$

We will use the state space model in its innovation form to explain the subspace algorithm for identifying combined deterministic-stochastic LTI systems.

2.2.3 Stability

2.2.4 Controlability and Observability

2.3 Linear Algebra Tools

2.3.1 Fundamental Matrix Subspaces

We require two of the fundamental matrix subspaces: the column space and the row space. The column space of a matrix $A \in \mathbb{R}^{m \times n}$ is the set of all linear combinations of the column vectors of A. The dimension of the column space is called the rank. The row space of a matrix $A \in \mathbb{R}^{m \times n}$ is the set of all linear combinations of the row vectors of A.

2.3.2 Projections

2.3.3 Singular Value Decomposition

Any matrix $A \in \mathbb{R}^{m \times n}$ can be decomposed by a singular value decomposition (SVD) given by

$$A = U \Sigma V^T$$

where $U \in \mathbb{R}^{m \times m}$ and $V \in \mathbb{R}^{n \times n}$ are orthogonal matrices and $\Sigma \in \mathbb{R}^{m \times n}$ is diagonal matrix of the singular values σ_i of A ordered such that

$$\sigma_1 \geq \sigma_2 \geq \cdots \geq \sigma_k > 0$$

2.3.4 Hankel Matrices

A Hankel matrix is a matrix $A \in \mathbb{R}^{m \times n}$ with constant skew-diagonals:

$$A_{m,n} = \begin{bmatrix} a_1 & a_2 & \cdots & a_n \\ a_2 & a_3 & \cdots & a_{n+1} \\ \vdots & \vdots & \ddots & \vdots \\ a_m & a_{m+1} & \cdots & a_{m+n-1} \end{bmatrix}$$

Hankel matrices can be constructed by setting the i, j^{th} element of A to

$$A_{i,j} = A_{i-1,j+1}$$

If each entry in the matrix is also a matrix, the resulting matrix is called a block Hankel matrix:

2.3.5 Toeplitz Matrices

A Toeplitz matrix is a matrix $A \in \mathbb{R}^{m \times n}$ with constant diagonals.

$$A_{m,n} = \begin{bmatrix} a_1 & a_{-1} & \cdots & a_{-n+1} \\ a_2 & a_1 & \ddots & \vdots \\ \vdots & \ddots & \ddots & a_{-1} \\ a_{m-1} & \cdots & a_2 & a_1 \end{bmatrix}$$

Topelitz matrices can be constructed by setting he i, j^{th} element of A to

$$A_{i,j} = A_{i+1,j+1}$$

2.4 Quadrotor Rigid Body Dynamics

CHAPTER 3

Subspace Identification Methods

Subspace identification methods (SIM) provide an approach to identifing LTI systems in their state space form using input-output data. SIMs provide an attractive alternative to Prediction Error Methods (PEM) because of their ability to identify MIMO systems and their non-iterative solution nature, making them suitable for working with large data sets. In general, the subspace identification problem is: given a set of input and output data, estimate the system matrices (A, B, C, D) up to within a similarity transform.

Extensive work in both the theory and application of SIMs in the last 20 years has resulted in the development of a number of popular algorithms, including the canonical variate analysis (CVA) method proposed by Larimore [10], the multi-variable output-error state space (MOESP) method proposed by Verhaegen [21], and the numerical algorithms for subspace state space system identification (N4SID) proposed by Van Overschee and De Moor [18]. A unifying theorem subsequently proposed by Van Overschee and De Moor [19] links these algorithms and provides a generalized approach to the subspace identification problem.

As described in Van Overschee and De Moor's unifying theorem, all SIMs follow the same general two step procedure. First, estimate the subspace spanned by the columns of the extended observability matrix (Γ_k) from input-output data u_k, y_k. Because the dimension of Γ_k determines the order n of the estimated system, a reduction of the system order is performed before proceeding. Second, the system matrices are determined, either directly from the extended observability matrix

or from the realized state sequence X_k.
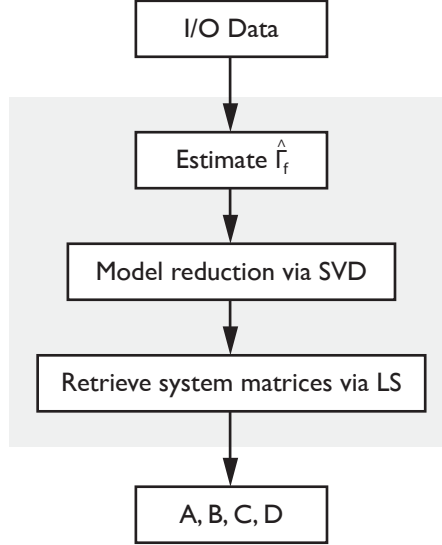
Figure 3.1: Subspace identification approach

3.1 Subspace System Identification

First, we consider the identification of a combined deterministic-stochastic LTI system operating in open loop. When a system is operating in open-loop (i.e. no feedback), the input data is assumed to be independent of past noise. In this case, the traditional SIMs (MOESP, N4SID, CVA) can be used without modification.
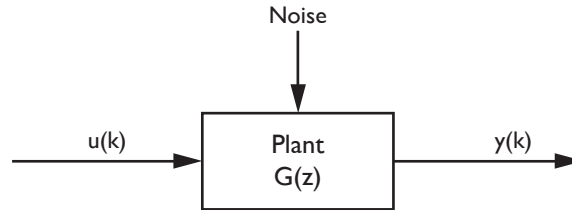
Figure 3.2: A block diagram of an LTI system operating in open loop.

3.1.1 Extended State Space Model

Recalling the combined deterministic-stochastic LTI system is given in its innovation form as

$$x(k+1) = Ax(k) + Bu(k) + Ke(k) \tag{3.1a}$$

$$y(k) = Cx(k) + Du(k) + e(k) \tag{3.1b}$$

Application of the subspace algorithms require we represent the input, output, and noise sequences in Hankel form with $2k$ block rows and N columns. For the input matrix,

$$U_k = \left[\begin{array}{cccc} u(0) & u(1) & \cdots & u(N-1) \\ u(1) & u(2) & \cdots & u(N) \\ \vdots & \vdots & \ddots & \vdots \\ u(k-1) & u(k) & \cdots & u(k+N-2) \\ \hline u(k) & u(k+1) & \cdots & u(k+N-1) \\ u(k+1) & u(k+2) & \cdots & u(k+N) \\ \vdots & \vdots & \ddots & \vdots \\ u(2k-1) & u(2k) & \cdots & u(2k+N-2) \end{array}\right] = \begin{bmatrix} U_p \\ U_f \end{bmatrix} \tag{3.2}$$

where p and f denote past and future horizons, respectively. The input matrix is partitioned into these two overlapping "past" and "future" blocks to later construct an instrumental variable matrix used to eliminate the influence of noise. We delay the explanation of this procedure until it is needed in Section 3.1.2. We construct similar matrices Y_k and E_k for the output and noise data.

Based on the state space representation in Eq. (3.1) and considering the future horizon, an extended state space model can be formulated as

$$Y_f = \Gamma_f X_k + H_f U_f + G_f E_f \tag{3.3}$$

The extended observability matrix is

$$\Gamma_f = \begin{bmatrix} C \\ CA \\ \vdots \\ CA^{f-1} \end{bmatrix} \tag{3.4}$$

and H_f and G_f are Toeplitz matrices of the Markov parameters of the deterministic and stochastic subsystems, respectively:

$$H_f = \begin{bmatrix} D & 0 & 0 & \cdots & 0 \\ CB & D & 0 & \cdots & 0 \\ CAB & CB & D & \cdots & 0 \\ \vdots & \vdots & \vdots & \ddots & \vdots \\ CA^{f-2}B & CA^{f-3}B & CA^{f-4}B & \cdots & D \end{bmatrix} \tag{3.5a}$$

$$G_f = \begin{bmatrix} I & 0 & 0 & \cdots & 0 \\ CK & I & 0 & \cdots & 0 \\ CAK & CK & I & \cdots & 0 \\ \vdots & \vdots & \vdots & \ddots & \vdots \\ CA^{f-2}K & CA^{f-3}K & CA^{f-4}K & \cdots & I \end{bmatrix} \tag{3.5b}$$

We will leverage this structure of Eq. (3.3) to identify the unknown system matrices from known input-output data. In particular, we will estimate the column space of the extended observability matrix. Knowledge of this subspace is sufficient to then recover the unknown system matrices.

3.1.2 Estimation of the Extended Observability Matrix

Determination of the system matrices relies on an estimate of the column space of Γ_f. In order to estimate the column space of Γ_f in Eq. (3.3), we must eliminate the influence of the input and noise terms. The general procedure, as outlined in

[13, 22] is as follows: First, we eliminate the influence of the input U_f by post-multiplying Eq. (3.3) by $\Pi_{U_f}^{\perp}$ where $\Pi_{U_f}^{\perp}$ is an orthogonal projection onto the column space of U_f given by

$$\Pi_{U_f}^{\perp} = I - U_f^T (U_f U_f^T)^{-1} U_f$$

By definition, $U_f \Pi_{U_f}^{\perp} = 0$ so Eq. (3.3) becomes

$$Y_f \Pi_{U_f}^{\perp} = \Gamma_f X_k \Pi_{U_f}^{\perp} + G_f E_f \Pi_{U_f}^{\perp} \tag{3.6}$$

Under open-loop conditions, E_f is uncorrelated with U_f. That is,

$$E_f \Pi_{U_f}^{\perp} = E_f (I - U_f^T (U_f U_f^T)^{-1} U_f) = E_f$$

so

$$Y_f \Pi_{U_f}^{\perp} = \Gamma_f X_k \Pi_{U_f}^{\perp} + G_f E_f \tag{3.7}$$

Next we eliminate the influence of the noise E_f. In order to remove the influence of the noise on the extended observability matrix, we must introduce an instrumental variable matrix as described in [22]. We seek a matrix $Z \in \mathbb{R}^{2k \times N}$ which exhibits the following properties:

$$\lim_{N \to \infty} \frac{1}{N} E_f Z^T = 0 \tag{3.8a}$$

$$\text{rank} \left(\lim_{N \to \infty} \frac{1}{N} X_k \Pi_{U_f}^{\perp} Z^T \right) = n \tag{3.8b}$$

Satisfying condition (3.8a) ensures that we can eliminate E_f by multiplying Eq. (3.7) on the right by Z^T and taking the limit for $N \to \infty$:

$$\lim_{N \to \infty} \frac{1}{N} Y_f \Pi_{U_f}^{\perp} Z^T = \lim_{N \to \infty} \frac{1}{N} \Gamma_f X_k \Pi_{U_f}^{\perp} Z^T \tag{3.9}$$

Satisfying condition (3.8b) ensures multiplication by Z^T does not change the rank of the remaining term on the right hand side of Eq. (3.9) so we have

$$\text{range} \left(\lim_{N \to \infty} \frac{1}{N} Y_f \Pi_{U_f}^{\perp} Z^T \right) = \text{range} \left(\Gamma_f \right) \tag{3.10}$$

13

From Eq. (3.10) we see that an SVD of the matrix $Y_f \Pi_{U_f}^{\perp} Z^T$ will provide an estimate of the column space of Γ_f. All that remains is to identify a suitable instrumental variable matrix Z. As described in [16, 22], instrumental variable matrices are typically constructed from input-output data. Recalling that we partitioned our input and output data into "past" and "future" sets in Section 3.1.1, we will use the "future" input-output data to identify the system and the "past" input-output data as the instrumental variable matrix Z_p:

$$Z_p = \begin{bmatrix} U_p \\ Y_p \end{bmatrix}$$

Recalling that E_f is uncorrelated with U_f for open-loop systems, and enforcing the assumption that E_f is white-noise, we have from [22] that

$$\lim_{N \to \infty} \frac{1}{N} E_f Z_p^T = 0$$

which satisfies condition (3.8a). Jannson showed in [6] that if the input sequence is persistently exciting, the rank condition (3.8b) is satisfied. We will enforce the persistence of excitation criteria during experiment design to ensure Z_p is a valid instrumental variable matrix.

3.1.3 Rank Reduction

In the presence of noise, the matrix $Y_f \Pi_{U_f}^{\perp} Z^T$ is full rank while the true system order is smaller. We choose the order of the identified system by partitioning the SVD matrices as follows:

$$Y_f \Pi_{U_f}^{\perp} Z^T = \begin{bmatrix} U_1 & U_2 \end{bmatrix} \begin{bmatrix} S_1 & 0 \\ 0 & S_2 \end{bmatrix} \begin{bmatrix} V_1^T & V_2^T \end{bmatrix}$$

where the number of singular values n in S_1 is equal to the system order and the remaining submatrices are scaled appropriately. The reduced rank estimate of the extended observability matrix is then

$$\hat{\Gamma}_f = U_1 S_1^{1/2} \tag{3.11}$$

3.1.4 Determination of the System Matrices

With an estimate of the column space of Γ_f, we are not able to recover the system matrices. In order to recover the system matrices, we follow the general procedure as outlined in [8]. First, we will exploit the structure of the extended observability matrix to recover the A and C matrices. The matrix C can be read directly from the first block row of $\hat{\Gamma}_f$. In order to recover A, we define the following two matrices

$$\hat{\overline{\Gamma}}_f = \begin{bmatrix} C \\ \vdots \\ CA^{f-2} \end{bmatrix}, \qquad \hat{\underline{\Gamma}}_f = \begin{bmatrix} CA \\ \vdots \\ CA^{f-1} \end{bmatrix} \tag{3.12}$$

where $\hat{\overline{\Gamma}}_f$ is equal to $\hat{\Gamma}_f$ without the last block row and $\hat{\underline{\Gamma}}_f$ is equal to $\hat{\Gamma}_f$ without the first block row. The structure of the matrices in Eq. (3.12) implies

$$\hat{\overline{\Gamma}}_f A = \hat{\underline{\Gamma}}_f \tag{3.13}$$

which is linear in A and can be solved by least squares.

All that remains is to recover the B and D matrices. Recalling the extended state space model is given by

$$Y_f = \Gamma_f X_k + H_f U_f + G_f E_f$$

and multiplying on the left by $\hat{\Gamma}_f^{\perp}$ and on the right by $U_f^{\dagger}$ we have

$$\hat{\Gamma}_f^{\perp} Y_f U_f^{\dagger} = \hat{\Gamma}_f^{\perp} \Gamma_f X_k U_f^{\dagger} + \hat{\Gamma}_f^{\perp} H_f U_f U_f^{\dagger} + \hat{\Gamma}_f^{\perp} G_f E_f U_f^{\dagger} \tag{3.14}$$

where $\hat{\Gamma}_f^{\perp}$ satisfies $\hat{\Gamma}_f^{\perp} \hat{\Gamma}_f = 0$ and $\dagger$ denotes the Moore-Penrose pseudoinverse. Equation (3.14) simplifies to

$$\hat{\Gamma}_f^{\perp} Y_f U_f^{\dagger} = \hat{\Gamma}_f^{\perp} H_f \tag{3.15}$$

Partitioning $\hat{\Gamma}_f^{\perp} Y_f U_f^{\dagger}$ into columns with the ith column denoted by $\mathcal{M}_i$ and $\hat{\Gamma}_f^{\perp}$

into rows with the jth row denoted by $\mathcal{L}_j$, Eq. (3.15) is

$$
\begin{bmatrix} \mathcal{M}_1 & \mathcal{M}_2 & \cdots & \mathcal{M}_f \end{bmatrix} = \begin{bmatrix} \mathcal{L}_1 \\ \mathcal{L}_2 \\ \vdots \\ \mathcal{L}_f \end{bmatrix} \begin{bmatrix} D & 0 & \cdots & 0 \\ CB & D & \cdots & 0 \\ \vdots & \vdots & \ddots & \vdots \\ CA^{f-2}B & CA^{f-3}B & \cdots & D \end{bmatrix}
$$

We can rewrite the above equation as

$$
\begin{bmatrix} \mathcal{M}_1 \\ \mathcal{M}_2 \\ \mathcal{M}_3 \\ \vdots \\ \mathcal{M}_f \end{bmatrix} = \begin{bmatrix} \mathcal{L}_1 & \mathcal{L}_2 & \cdots & \mathcal{L}_{f-1} & \mathcal{L}_f \\ \mathcal{L}_2 & \mathcal{L}_3 & \cdots & \mathcal{L}_f & 0 \\ \mathcal{L}_3 & \mathcal{L}_4 & \cdots & 0 & 0 \\ \vdots & \vdots & \ddots & \vdots & \vdots \\ \mathcal{L}_f & 0 & 0 & \cdots & 0 \end{bmatrix} \begin{bmatrix} I & 0 \\ 0 & \hat{\Gamma}_f \end{bmatrix} \begin{bmatrix} D \\ B \end{bmatrix} \tag{3.16}
$$

which is an overdetermined linear system in B and D. We recover B and D through least squares with $B \in \mathbb{R}$???

3.1.5 Determination of the Kalman Filter Gain

3.1.6 Numerical Efficiencies by LQ Factorization

In the case where N is large, the construction of the matrix $Y_f \Pi_{U_f}^{\perp} Z^T$ in Eq. (3.10) and the subsequent calculation of its SVD are computationally intensive. Verhaegen has shown in [20] that from the following LQ factorization

$$
\begin{bmatrix} U_f \\ U_p \\ Y_p \\ Y_f \end{bmatrix} = \begin{bmatrix} L_{11} & 0 & 0 & 0 \\ L_{21} & L_{22} & 0 & 0 \\ L_{31} & L_{32} & L_{33} & 0 \\ L_{41} & L_{42} & L_{43} & L_{44} \end{bmatrix} \begin{bmatrix} Q_1 \\ Q_2 \\ Q_3 \\ Q_4 \end{bmatrix} \tag{3.17}
$$

we have

$$
\text{range}\left(\lim_{N \to \infty} \frac{1}{\sqrt{N}} \begin{bmatrix} L_{42} & L_{43} \end{bmatrix} \right) = \text{range}\left(\Gamma_f \right) \tag{3.18}
$$

16

This shows an equivalency between Eq. (3.10) and Eq. (3.18), therefore we can estimate the column space of $\hat{\Gamma}_f$ by computing the LQ factorization in Eq. (3.17), taking the SVD of the matrix $\begin{bmatrix} L_{42} & L_{43} \end{bmatrix}$, and reducing the system order as described above. The remainder of this document assumes $\hat{\Gamma}_f$ is estimated via LQ factorization.

3.2   Closed-Loop Subspace Identification

In many real-world situations, it is either not practical or not possible to collect open-loop input and output data. An unstable system relying on some form of feedback control to operate safely is an example of such a case. It is well known that traditional subspace methods produce biased results in the presence of feedback. This is due to the correlation between the system input and past noise as the controller attempts to eliminate system disturbances [13]. As a result, traditional SIMs are not albe to fully decouple the input and noise sequences when estimating the subspace of the extended observability matrix.
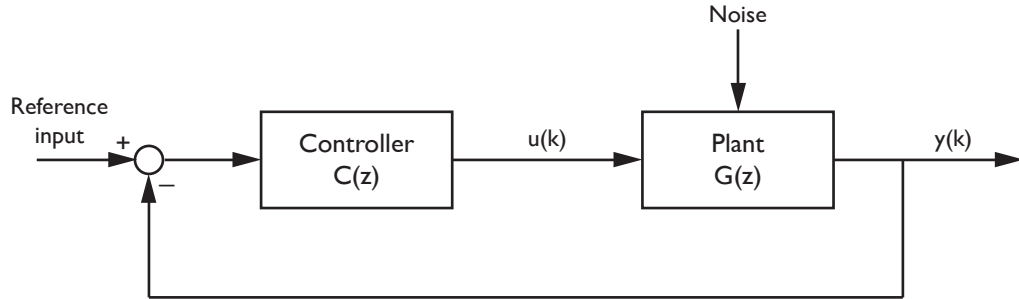

Figure 3.3: A block diagram of an LTI system operating under feedback control.

Recently, several new approaches to identifying closed-loop systems by decoupling inputs from past noise (thus removing any bias) have been proposed. Among these approaches are the Innovation Estimation Method (IEM) proposed by Qin and Ljung [14] and the Whitening Filter Approach (WFA) proposed by Chiuso

and Picci [3]. The IEM pre-estimates the innovation sequence E_f row-wise via a high-order Auto-Regression model with eXogeneous inputs (ARX) algorithm, which is then used to estimate Γ_f from Eq. (3.3). The WFA partitions a modified version of the extended state space model row-wise and estimates Γ_f through a multi-stage least squares followed by an SVD. It is worth noting that Chiuso and Picci concluded in [3] that while all closed-loop subspace identification algorithms considered produce somewhat biased results in the presence of feedback control, these algorithms are still able to provide significant improvements over traditional SIMs when identifying closed-loop systems.

3.2.1 Estimation of the Extended Observability Matrix by the Whitening Filter Approach

In order to describe the Whitening Filter Approach, we introduce the predictor form of the system:

$$x(k+1) = A_K x(k) + B_K u(k) + K y(k) \tag{3.19a}$$

$$y(k) = Cx(k) + Du(k) + e(k) \tag{3.19b}$$

where $A_K = A - KC$ and $B_K = B - KD$. Because the input $u(k)$ is determined via feedback, we consider it to be correlated with past innovation $e(k)$. The state $x(k)$ of this form is the same as for the innovation form in Eq. (2.4), but because A_K is guaranteed stable even if the original process matrix A is unstable, the predictor form proves advantageous when considering open-loop unstable systems [13].

We are able to derive an expression for X_k by iterating Eq. (3.19)

$$X_k = L_p Z_p + A_K^p X_{k-p} \tag{3.20}$$

where

$$X_k = \begin{bmatrix} x(k) & x(k+1) & \cdots & x(k+N-1) \end{bmatrix}$$

$$L_p = \begin{bmatrix} L_p^y & L_p^u \end{bmatrix}$$

$$L_p^u = \begin{bmatrix} A_K^{p-1}B_K & A_K^{p-2}B_K & \cdots & B_K \end{bmatrix}$$

$$L_p^y = \begin{bmatrix} A_K^{p-1}K & A_K^{p-2}K & \cdots & K \end{bmatrix}$$

$$Z_p = \begin{bmatrix} Y_p^T & U_p^T \end{bmatrix}^T$$

Based on the state space representation in Eq. (3.19), we construct the following modified state space model

$$Y_f = \overline{\Gamma}_f X_k + \overline{H}_f U_f + \overline{G}_f Y_f + E_f \tag{3.21}$$

with a modified extended observability matrix given by

$$\overline{\Gamma}_f = \begin{bmatrix} C \\ CA_K \\ \vdots \\ CA_K^{f-1} \end{bmatrix} \tag{3.22}$$

and Toeplitz matrices $\overline{H}_f$ and $\overline{G}_f$ given by

$$\overline{H}_f = \begin{bmatrix} D & 0 & 0 & \cdots & 0 \\ CB_K & D & 0 & \cdots & 0 \\ CA_KB_K & CB_K & D & \cdots & 0 \\ \vdots & \vdots & \vdots & \ddots & \vdots \\ CA_K^{f-2}B_K & CA_K^{f-3}B_K & CA_K^{f-4}B_K & \cdots & D \end{bmatrix} \tag{3.23a}$$

$$\overline{G}_f = \begin{bmatrix} 0 & 0 & 0 & \cdots & 0 \\ CK & 0 & 0 & \cdots & 0 \\ CA_KK & CK & 0 & \cdots & 0 \\ \vdots & \vdots & \vdots & \ddots & \vdots \\ CA_K^{f-2}K & CA_K^{f-3}K & CA_K^{f-4}K & \cdots & 0 \end{bmatrix} \tag{3.23b}$$

19

Substituting Eq. (3.20) into Eq. (3.21), we have

$$Y_f = \overline{\Gamma}_f L_p Z_p + \overline{\Gamma}_f A_K^p X_{k-p} + \overline{H}_f U_f + \overline{G}_f Y_f + E_f \tag{3.24}$$

If we assume that the eigenvalues of A_K lie strictly within the unit circle, for a sufficiently large p, $A_K^p \approx 0$ so Eq. (3.24) becomes

$$Y_f = \overline{\Gamma}_f L_p Z_p + \overline{H}_f U_f + \overline{G}_f Y_f + E_f \tag{3.25}$$

Partitioning Eq. (3.25) row-wise, we have

$$Y_{fi} = \overline{\Gamma}_{fi} L_p Z_p + \overline{H}_{fi} U_{fi} + \overline{G}_{fi} Y_{fi} + E_{fi} \tag{3.26}$$

where

$$\overline{\Gamma}_{fi} = C A_K^{i-1}$$
$$\overline{H}_{fi} = \begin{bmatrix} C A_K^{i-2} B_K & C A_K^{i-3} B_K & \cdots & C B_K & D \end{bmatrix}$$
$$\overline{G}_{fi} = \begin{bmatrix} C A_K^{i-2} K & C A_K^{i-3} K & \cdots & C K & 0 \end{bmatrix}$$

Using least squares, we estimate $\overline{\Gamma}_{fi} L_p$ for $i = 1, 2, \ldots, f$, which then forms $\widehat{\overline{\Gamma}_f L_p}$

CHAPTER 4

Approach

4.1 Quadrotor Platform

Because the design and construction of a quadrotor is beyond the scope of this project, we will use a commercially available vehicle called the Bitcraze Crazyflie [1]. The Crazyflie, shown in Figure 4.1 is a small, low cost, open-source quadrotor kit suitable for indoor flight. It measures 9 cm motor to motor and weighs 19 grams. A 170 mAh lithium-polymer battery powers the vehicle, providing 7 minutes of flight time. An onboard microcontroller is responsible for vehicle stabilization and control and reads sensor measurements from a three-axis accelerometer, three-axis gyroscope, three-axis magnetometer, and barometer.

Vehicle pitch, roll, yaw, and thrust inputs are set in one of two ways. First, a USB gamepad connected to a computer running the Crazyflie PC client provides a method for direct user control of the vehicle. Second, the PC client exposes a Python API, making it possible to programmatically send the vehicle control setpoints. The vehicle receives control inputs and transmits telemetry data wirelessly over a 2.4 GHz radio connection to a USB radio dongle connected to the Crazyflie PC client running on a laptop computer.

4.2 Experiment Design
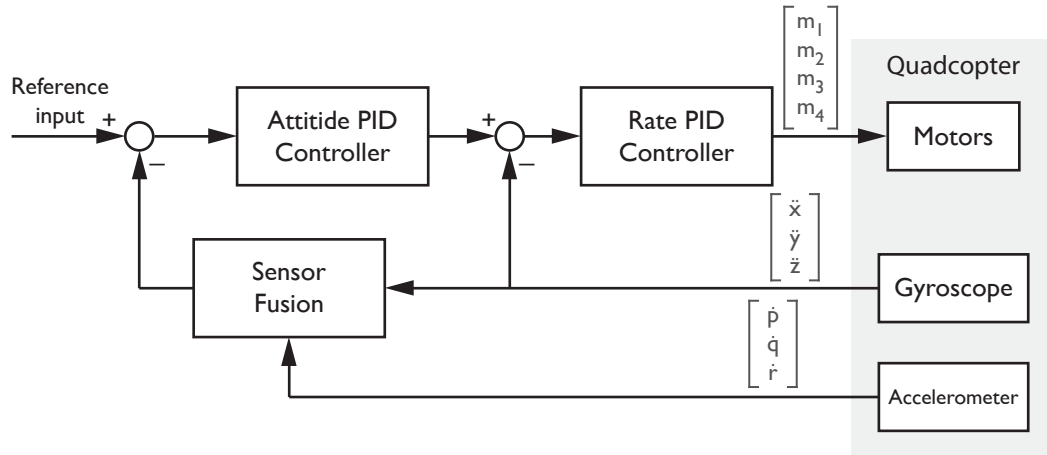
blah

Figure 4.1: Bitcraze Crazyflie Quadrotor

Figure 4.2: Crazyflie control system block diagram

4.3   Data Collection

4.4   Data Analysis

INCLUDE OVERVIEW OF WFA ALGORITHM IN BOX (MATH-BASED) IN
THIS SECTION   22

4.5   Verification

CHAPTER 5

Results

CHAPTER 6

Conclusion

6.1 Future Work

References

[1] Bitcraze. http://www.bitcraze.se, 2013.

[2] Anthony RS Bramwell, David Balmford, and George Done. *Bramwell's helicopter dynamics.* Butterworth-Heinemann, 2001.

[3] Alessandro Chiuso and Giorgio Picci. Consistency analysis of some closed-loop subspace identification methods. *Automatica*, 41(3):377–391, 2005.

[4] Shweta Gupte, Paul Infant Teenu Mohandas, and James M Conrad. A survey of quadrotor unmanned aerial vehicles. In *Southeastcon, 2012 Proceedings of IEEE*, pages 1–6. IEEE, 2012.

[5] Gabriel M Hoffmann, Haomiao Huang, Steven L Waslander, and Claire J Tomlin. Quadrotor helicopter flight dynamics and control: Theory and experiment. In *Proc. of the AIAA Guidance, Navigation, and Control Conference*, pages 1–20, 2007.

[6] Magnus Jansson. On subspace methods in system identification and sensor array signal processing. *These de doctorat-Royal institute of technology, Stockholm*, 1997.

[7] Rudolph Emil Kalman et al. A new approach to linear filtering and prediction problems. *Journal of basic Engineering*, 82(1):35–45, 1960.

[8] Tohru Katayama. *Subspace methods for system identification.* Springer, 2005.

[9] Arda Özgür Kivrak. Design of control systems for a quadrotor flight vehicle equipped with inertial sensors. *Atilim University, December*, 2006.

[10] Wallace E Larimore. Canonical variate analysis in identification, filtering, and adaptive control. In *Decision and Control, 1990., Proceedings of the 29th IEEE Conference on*, pages 596–604. IEEE, 1990.

[11] Daniel Mellinger, Michael Shomin, and Vijay Kumar. Control of quadrotors for robust perching and landing. In *Proc. Int. Powered Lift Conf*, pages 119–126, 2010.

[12] Nathan Michael, Daniel Mellinger, Quentin Lindsey, and Vijay Kumar. The grasp multiple micro-uav testbed. *Robotics & Automation Magazine, IEEE*, 17(3):56–65, 2010.

[13] S Joe Qin. An overview of subspace identification. *Computers & chemical engineering*, 30(10):1502–1513, 2006.

[14] S Joe Qin and Lennart Ljung. Closed-loop subspace identification with innovation estimation. In *Proceedings of SYSID*, volume 2003, 2003.

[15] Zak Sarris and STN ATLAS. Survey of uav applications in civil markets (june 2001). In *The 9 th IEEE Mediterranean Conference on Control and Automation (MED'01)*, 2001.

[16] Torsten Söderström and Petre Stoica. *Instrumental variable methods for system identification*, volume 161. Springer-Verlag Berlin, 1983.

[17] Kimon P Valavanis. *Advances in unmanned aerial vehicles: state of the art and the road to autonomy*, volume 33. Springer, 2007.

[18] Peter Van Overschee and Bart De Moor. N4sid: Subspace algorithms for the identification of combined deterministic-stochastic systems. *Automatica*, 30(1):75–93, 1994.

[19] Peter Van Overschee and Bart De Moor. A unifying theorem for three subspace system identification algorithms. *Automatica*, 31(12):1853–1864, 1995.

[20] Michel Verhaegen. Identification of the deterministic part of mimo state space models given in innovations form from input-output data. *Automatica*, 30(1):61–74, 1994.

[21] Michel Verhaegen and Patrick Dewilde. Subspace model identification part 1. the output-error state-space model identification class of algorithms. *International journal of control*, 56(5):1187–1210, 1992.

[22] Michel Verhaegen and Vincent Verdult. *Filtering and system identification: a least squares approach*. Cambridge university press, 2007.

[23] Mats Viberg. Subspace-based methods for the identification of linear time-invariant systems. *Automatica*, 31(12):1835–1851, 1995.